Eur. Phys. J. B **28**, 55–60 (2002)
DOI: 10.1140/epjb/e2002-00199-4

THE EUROPEAN PHYSICAL JOURNAL B

Non-Fermi liquid behavior in the stripe phase of the extended Hubbard model

R. Citro[a] and M. Marinaro

Dipartimento di Fisica "E.R. Caianiello", Università di Salerno and Unità INFM di Salerno Via S. Allende, 84081 Baronissi (Sa), Italy

Received 28 February 2002 / Received in final form 7 May 2002
Published online 9 July 2002 –

Abstract. Within a strong-coupling perturbative approach, based on a Cumulant Expansion of the extended single-band Hubbard model, we show that the on-shell inverse scattering time deviates from the normal Fermi-liquid behavior near the points of the Fermi surface connected by the characteristic wavevector of an incommensurate charge density wave. The violation of the Fermi liquid behavior is associated with a square root behavior of the inverse quasiparticle lifetime in proximity of a stripe phase. Some relevant features observed in ARPES experiments on Bi2212 are qualitatively reproduced.

PACS. 74.20.-z Theories and models of superconducting state – 71.45.Lr Charge-density-wave systems – 71.10.Hf Non-Fermi-liquid ground states, electron phase diagrams and phase transitions in model systems

1 Introduction

Understanding transport in the cuprates superconductors is one of the central issue in solid state physics. Many experimental results obtained by different techniques, as angle resolved photoemission (ARPES) and neutron diffraction (NMR), have shown that the normal state of the high temperature superconductors (HTS) is not a conventional Fermi liquid [2]. Signatures of a Fermi liquid behavior are observed in the heavily overdoped cuprates, while deviations from the standard Fermi liquid emerge at lower doping. Near optimal doping the non-Fermi liquid behavior is characterized by a $1/\omega$ conductivity [3] and a linear T resistivity [4,5]. Furthermore, in this region various experiments highlight the formation of local, self-organized quasi-one-dimensional structures, "stripes", which substantially affect low-energy excitations [6–9]. Two characteristic features that emerge in ARPES experiments on optimally doped $Bi_2Sr_2CaCu_2O_{8+\delta}$ (Bi2212) are a linear behavior of the inverse lifetime at the Fermi level over a wide range of temperature [1] and an asymmetric suppression of the spectral weight at the points of the Fermi surface connected by an incommensurate wavevector $Q_c = (0.4\pi/a, -0.4\pi/a)$ [10,11], interpretable as a signature of quasi-critical charge fluctuations close to a stripe phase. From these findings, arises the speculation that the elementary excitations in this material might be drastically different from those in traditional metals where the Fermi liquid theory has proved most successful [2]. To explain both the observed linearities in the transport properties [12–14] and the origin of the stripe phase near optimal doping [15,16], different scenarios have been proposed. A common idea is that the origin of non-Fermi-liquid (NFL) behavior is related to the presence of a *quantum critical point* (QCP) [17] at optimal doping, *i.e.* a phase transition at zero temperature driven by quantum fluctuations of some kind (charge, spin, etc.) rather than thermal fluctuations. The possibility of a quantum critical behavior has recently been discussed in several models of high-T_c superconductivity [12,16]. One possible realization of this scenario is based on an incommensurate charge-density-wave (ICDW) instability that gives rise to a singularity in the effective scattering amplitude among quasiparticles near the Fermi surface (FS) [16]. Assuming the possibility of a singular scattering, various experimental results were explained [18] in a phenomenological model of fermions coupled to a charge vertex, as the linear-in-T resistivity and the presence of shadow-bands in the single-particle spectra of Bi2212.

In this paper, we present a microscopic analysis of quasiparticles lifetime in the stripe-phase of the 2D single-band Hubbard model generalized with the inclusion of a non-local (long-range) Coulomb interaction, to understand the role of critical charge fluctuations on the deviation from Fermi liquid behavior observed into experiments. Employing a *strong-coupling* approach based on a Cumulant Expansion (CE), we derive an analytic expression for the quasiparticles lifetime in terms of a charge vertex in the normal phase. This allows us to study the influence of the charge vertex singularity on the behavior of the quasiparticles lifetime around the FS. We find that in a suitable range of doping, the vertex presents a singularity,

[a] e-mail: citro@sa.infn.it

at a finite wavevector, of the type introduced phenomenologically in reference [18], signalling an instability towards an ICDW. It is shown that, near the singularity, a linear behavior of $\mathrm{Im}\Sigma(\omega)$ emerges in the crossover regime between a Fermi liquid at higher doping and low temperature (where $\mathrm{Im}\Sigma \propto \omega^2$) and the quantum-critical regime where $\mathrm{Im}\Sigma \propto \sqrt{\omega}$. The crossover between the two limits is governed by a single parameter, *i.e.* the inverse squared of the correlation length, $\xi^{-2} \sim a(\delta - \delta_c)$, that locates at a critical doping $\delta = \delta_c$ the stripe phase transition.

The organization of the paper is the following. In Section 2 we introduce the model and derive an expression for the quasiparticles lifetime in terms of the charge vertex function. In Section 3 we discuss the results for the lifetime as a function of the doping and comment on the deviations from a standard Fermi-liquid behavior, comparing with experiments. Finally, we draw the conclusions in Section 4.

2 Inverse scattering time of quasiparticles in proximity of a stripe phase

The Hamiltonian of the 2D single-band Hubbard model generalized with the inclusion of a non-local (long-range) Coulomb interaction, is given by:

$$H = \sum\nolimits_{\langle i,j\rangle',\sigma} t_{ij} c^{\dagger}_{i\sigma} c_{j\sigma} - \mu \sum\nolimits_{\sigma} n_{i\sigma} + U \sum_{i} n_{i\uparrow} n_{i\downarrow} + \sum_{i,j} V_{i,j} n_i n_j, \quad (1)$$

where $c^{\dagger}_{i\sigma}(c_{i\sigma})$ is an electron creation (annihilation) operator with spin σ at site i, t_{ij} denotes the hopping up to next-to-nearest included, μ is the chemical potential, U and $V_{i,j}$ represent the local and the long-range Coulomb interaction, respectively, and $n_i = (n_{i\uparrow} + n_{i\downarrow})$. $V_{i,j}$ represents the Coulombic potential between the electrons on a two-dimensional square lattice embedded in a three dimensional space with a separation d between the plane in z direction.

The model is treated by a strong-coupling perturbative approach, based on a Cumulant Expansion (CE) [19,20], that consists in taking the local-Coulomb term in the unperturbed Hamiltonian and introducing the non-local terms as perturbations. This expansion is equivalent to a nonstandard diagram technique [19–21] that permits to evaluate the one-particle Green's function *via* a Dyson-like equation.

Within this approach, in a recent paper [22] we have computed the charge-vertex function of model (1) in the normal phase to investigate the existence of a charge instability. The analysis at low energy and low-temperature of the vertex function reveals that when, only the local Coulomb repulsion is taken into account, a divergence at the wavevector $\mathbf{q} = \mathbf{0}$ drives the system towards a phase separation (PS) while an incommensurate charge density wave (ICDW) develops when nonlocal Coulomb interactions are included. This instability is associated to a stripe phase. While the stripe formation can be explained by the vertex singularity at a finite wavevector $\mathbf{q} \neq \mathbf{0}$, a measure of the violation of the normal FL behavior is provided by the behavior of the quasiparticle lifetime around the singularity.

The on-shell lifetime of a quasiparticle $\tau_{\mathbf{k}}$ at $T = 0$ is related to the imaginary part of the self-energy, and of course of the total Green's function, by the relation:

$$\frac{1}{\tau_{\mathbf{k}}} = -\frac{1}{\pi}\mathrm{Im}\Sigma(\mathbf{k}, \epsilon_{\mathbf{k}}) = -\frac{1}{\pi}\mathrm{Im}G^{-1}(\mathbf{k}, \epsilon_{\mathbf{k}}). \quad (2)$$

where we have put $G_{\sigma}(\mathbf{k}, \epsilon_{\mathbf{k}}) = G_{-\sigma}(\mathbf{k}, \epsilon_{\mathbf{k}}) = G(\mathbf{k}, \epsilon_{\mathbf{k}})$.

Within the Cumulant Expansion approach, the one-particle Green's function $G(\mathbf{k}, \mathrm{i}\omega_n)$ is given by

$$G(\mathbf{k}, \mathrm{i}\omega_n) = \frac{[G^0(\mathrm{i}\omega_n) + Z(\mathbf{k}, \mathrm{i}\omega_n)]}{1 - t(\mathbf{k})[G^0(\mathrm{i}\omega_n) + Z(\mathbf{k}, \mathrm{i}\omega_n)]}, \quad (3)$$

where $G^{(0)}(\mathrm{i}\omega_n)$ is the local-Hubbard Green's function and the function $Z(\mathbf{k}, \mathrm{i}\omega_n)$ contains all the irreducible graphs with two insertions which cannot be broken into two parts by cutting a single line hopping, finally $t(\mathbf{k}) = -2t(\cos k_x + \cos k_y) + 4t' \cos k_x \cos k_y$. Explicitly,

$$G^{(0)}(\mathrm{i}\omega_n) = \frac{1 - \langle n\rangle}{\mathrm{i}\omega_n + \mu} + \frac{\langle n\rangle}{\mathrm{i}\omega_n - (U - \mu)}, \quad (4)$$

where $\langle n\rangle$ is the averaged on-site density of electrons per spin.

From the analytic continuation ($\mathrm{i}\omega_n \to \omega + \mathrm{i}\eta$) of equation (3) we get

$$\mathrm{Im}G^{-1}(\mathbf{k}, \omega) = \frac{\mathrm{Im}Z(\mathbf{k}, \omega)}{(\mathrm{Re}G^0(\omega) + \mathrm{Re}Z(\mathbf{k}, \omega))^2 + (\mathrm{Im}Z(\mathbf{k}, \omega))^2}. \quad (5)$$

The evaluation of the inverse scattering time is based on the calculation of real and imaginary part of the function $Z(\mathbf{k}, \omega)$. In the approximation in which we neglect cumulants of order greater than two, the function $Z(\mathbf{k}, \omega)$ is diagrammatically shown in Figure 1 and its analytical expression is the following:

$$Z(\mathbf{k}, \mathrm{i}\omega_n) = -2\beta^{-1} \sum_{k'} \Gamma(kk', kk') G^{(1)}(k') t^2_{\mathbf{k}'} + \beta^{-1} \sum_{k'} \Gamma(kk', k'k) G^{(1)}(k') t^2_{\mathbf{k}'}. \quad (6)$$

Here we have introduced the shorthand notation $k = (\mathbf{k}, \mathrm{i}\omega_n)$, and the 2 comes from the spin. $G^{(1)}(k)$ is the one-particle Green's function obtained in the lowest order CE [23] and $\Gamma(kk', kk')$ is the effective interaction between quasiparticles, *i.e.* the vertex function. The diagram structure we have considered is equivalent to a one-loop self-energy approximation. Graph (a) corresponds to a direct scattering while graph (b) to an exchange scattering in which one must take into account only those background particles which have a spin whose projection coincides

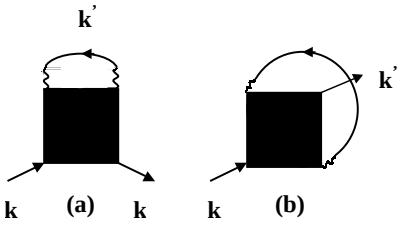

Fig. 1. Proper self-energy. Graph (a) represents the direct scattering while (b) the exchange scattering. The wavy line is the hopping $t_{\mathbf{k}}$, the line straight line represents the one-particle Green's function obtained in the lowest order CE and the square is the effective interaction potential $\Gamma(\mathbf{k}, \mathrm{i}\omega_n)$.

with the projection of the impinging particle spin. The explicit expression of $G^{(1)}(\mathbf{k}, \mathrm{i}\omega_n)$, is

$$G^{(1)}(\mathbf{k}, \mathrm{i}\omega_n) = \frac{G^{(0)}(\mathrm{i}\omega_n)}{1 - t(\mathbf{k})G^{(0)}(\mathrm{i}\omega_n)} = \sum\nolimits_{i=1,2} \frac{A_i(\mathbf{k})}{\mathrm{i}\omega_n - \varepsilon_i(\mathbf{k})}, \tag{7}$$

where $\varepsilon_i(\mathbf{k})$ ($i = 1, 2$) is the energy spectrum consisting of two Hubbard subbands:

$$\varepsilon_{1,2}(\mathbf{k}) = \frac{1}{2}[(U - 2\mu) + t(\mathbf{k}) \mp \sqrt{(U - t(\mathbf{k}))^2 + 4t(\mathbf{k})\langle n\rangle U}], \tag{8}$$

$A_i(\mathbf{k})$ ($i = 1, 2$) are the residues at each pole:

$$A_1(\mathbf{k}) = \frac{\varepsilon_1(\mathbf{k}) - U(1 - \langle n\rangle)}{\varepsilon_1(\mathbf{k}) - \varepsilon_2(\mathbf{k})} = 1 - A_2(\mathbf{k}). \tag{9}$$

The vertex $\Gamma(kk', kk')$ is obtained by the summation of ladder type of diagrams in the particle-hole channel shown in Figure 2, where the square denotes, as usual, the Feynman diagrams assembly describing the effective interaction of two particles. We neglect the contribution from the particle-particle channel, *i.e.* the superconducting fluctuations. The empty square corresponds to the bare vertex function $\Gamma^{(0)}(\mathrm{i}\omega_n)$, whose explicit expression can be found in reference [22]. These diagrams have the usual structure of a Random Phase Approximation (RPA) and can be summed *via* a Bethe-Salpeter equation [24]. The difference between the classical RPA and our generalized RPA consists in the character of the bare vertex that in our case is *a two-particle cumulant* instead of a spatially local non-retarded interaction.

In the approximation in which the effective scattering potential is a function of the longitudinal transfer momentum only, equation (6) becomes:

$$Z(\mathbf{k}, \mathrm{i}\omega_n) = -\beta^{-1} \sum_{\omega_{n'}} \sum_{\mathbf{k}'} \Gamma(\mathbf{k}', \mathrm{i}\omega_{n'}) \times G^{(1)}(\mathbf{k} - \mathbf{k}', \mathrm{i}\omega_n - \mathrm{i}\omega_{n'}) t^2_{\mathbf{k}-\mathbf{k}'}. \tag{10}$$

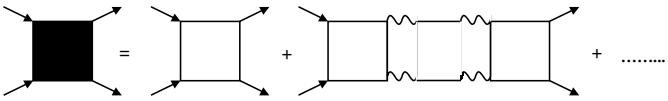

Fig. 2. Bethe-Salpeter equation for the effective interaction in the ladder approximation. The bare square is a second order cumulant Γ^0 describing the local interaction of two particles. The arrow indicates the direction of increasing time, while along the vertical direction equal times are considered.

If $V_{i,j} = 0$, *i.e.* in absence of non-local Coulomb repulsion, the charge vertex is given by [24]:

$$\Gamma(\mathbf{k}, \mathrm{i}\omega_n) = \Gamma^{(0)}(\mathrm{i}\omega_n) + \Gamma^{(0)}(\mathrm{i}\omega_n)\Pi(\mathbf{k}, \mathrm{i}\omega_n)\Gamma(\mathbf{k}, \mathrm{i}\omega_n), \tag{11}$$

where $\Pi(\mathbf{k}, \mathrm{i}\omega_n)$ is the polarization insertion

$$\Pi(\mathbf{k}, \mathrm{i}\omega_n) = 2\widetilde{t}(\mathbf{k}) - \frac{2}{\beta} \sum\nolimits_{\mathbf{q}, \mathrm{i}\omega'_n} t^2_{\mathbf{k}+\mathbf{q}} t^2_{\mathbf{q}} \times G^{(1)}(\mathbf{k} + \mathbf{q}, \mathrm{i}\omega_n + \mathrm{i}\omega'_n) G^{(1)}(\mathbf{q}, \mathrm{i}\omega_n), \tag{12}$$

$\widetilde{t}(\mathbf{k}) = 2(\cos k_x + \cos k_y) + 4t'^2 \cos k_x \cos k_y$ [25] is the analytic expression for the bubble made up of two hopping lines only. As shown in reference [22], when we add a long-range (LR) Coulomb interaction the long-range vertex, Γ^{LR}, is expressed in terms of the short-range vertex (11), denoted by Γ^{SR}, by the following relation:

$$\Gamma^{LR}(\mathbf{k}, \mathrm{i}\omega_n) = \frac{\Gamma^{(0)}(\mathrm{i}\omega_n)}{1 - \Gamma^{(0)}(\mathrm{i}\omega_n)\left(\Pi(\mathbf{k}, \mathrm{i}\omega_n) + V(\mathbf{k})\right)} = \frac{\Gamma^{SR}(\mathbf{k}, \mathrm{i}\omega_n)}{1 - \Gamma^{SR}(\mathbf{k}, \mathrm{i}\omega_n)V(\mathbf{k})}. \tag{13}$$

where $V(\mathbf{k})$ is the Fourier transform of $V_{i,j}$, $V(\mathbf{k}) = VG(\mathbf{q})$, $V = e^2 d/(2\epsilon_\perp a^2)$ is the Coulombic coupling constant and $G(\mathbf{q}) = \frac{1}{\sqrt{A^2(\mathbf{q})-1}}$, $A(\mathbf{q}) = [\varepsilon_\parallel/(\varepsilon_\perp a^2/d^2)][(\cos(aq_x)+\cos(aq_y)-2)-1]$, a is the lattice spacing, d is the separation between the planes along the z-direction and $\varepsilon_{\parallel(\perp)}$ indicates the dielectric constant parallel (perpendicular) to the plane [26]. In the following we assume typical values of the parameters of copper oxide superconductors in the normal phase, *i.e.* $d \simeq 3a$, $\varepsilon_\perp \simeq 5$ and $\varepsilon_\parallel \simeq 30$. Hereon we will consider the long-range vertex only that we simply denote by Γ for brevity.

After the analytic continuation in (10) we obtain that the retarded Z function is given by:

$$Z(\mathbf{k}, \omega) = \sum_{\mathbf{k}'} \int \frac{\mathrm{d}\omega'}{2\pi} t^2_{\mathbf{k}-\mathbf{k}'} [n_B(\omega')\mathrm{Im}\Gamma(\mathbf{k}', \omega') \times G^{\mathrm{A}}(\mathbf{k} - \mathbf{k}', \omega - \omega') - n_F(\omega') \times \Gamma(\mathbf{k}', \omega - \omega')\mathrm{Im}G^{\mathrm{R}}(\mathbf{k} - \mathbf{k}', \omega')], \tag{14}$$

where the superscript A(R) refers to the advanced (retarded) Green's function. The imaginary part of (14) is:

$$\mathrm{Im}Z(\mathbf{k},\omega) = -\pi \sum_{\mathbf{k}'} \int \frac{\mathrm{d}\omega'}{2\pi} A_{\mathbf{k}-\mathbf{k}'} t^2_{\mathbf{k}-\mathbf{k}'} \mathrm{Im}\Gamma(\mathbf{k}',\omega') \times [n_B(\omega') + n_F(\epsilon_{\mathbf{k}-\mathbf{k}'})]\delta(\omega - \omega' - \epsilon_{\mathbf{k}-\mathbf{k}'}). \quad (15)$$

The kernel of the integral (15), can be evaluated by using the low-energy expression for the vertex function (13). As we have shown in a recent work [22], in the low-energy limit we have

$$\Gamma(\mathbf{k}',\omega' \to 0) \simeq -\frac{1}{\Omega(\mathbf{k}') - \mathrm{i}\gamma_{k'}\omega'}, \quad (16)$$

where $\gamma_{k'}$ is the inverse relaxation time of the charge fluctuation, $\Omega(\mathbf{k}')$ goes to zero for $\mathbf{k}' = 0$ in the case $V(\mathbf{k}') = 0$ (local interaction only), while for $V(\mathbf{k}') \neq 0$, $\Omega(\mathbf{k}')$ has been studied numerically and presents a zero for $\mathbf{k}' = \mathbf{q_c} \neq 0$. As $\omega' \to 0$, the zeros of $\Omega(\mathbf{k}')$ determine completely the singular behavior of the vertex function. There are different ways in which Γ can diverge and the trend of the physical quantities depend strongly on the type of singularity. In a previous work [22], being interested only in the stripe formation induced by the long-range Coulomb interaction, we have computed the critical wavevector $\mathbf{q_c}$ along the instability line $\Gamma(\mathbf{k}',0)^{-1} = 0$, by looking at the values of $\mathbf{q_c}$ where $V(\mathbf{k}')$ takes the smallest value [27]. This has lead to a linear type of divergence, *i.e.* governed by $\Omega(\mathbf{k}') \simeq a + b(\mathbf{k}' - \mathbf{q_c})$, where a depends on doping and b is a constant.

Here, in order to have a more complete correspondence with the experimental findings, we are interested to look for a singularity of Γ which is consistent with a quantum critical behaviour of a Gaussian type [17], $\Gamma(\mathbf{k}',0) \simeq -1/(M^2 + (k'_x - q_{xc})^2 + (k'_y - q_{yc})^2)$ for $\mathbf{k}' \to \mathbf{q_c}$. Numerical results show that for physical values of (U,V,δ) there exists a value $\mathbf{q_c}$ such that $\Omega(\mathbf{k}') \simeq M(\delta) + \alpha(\mathbf{k} - \mathbf{q_c})^2$, where $\xi^{-2} = M(\delta)$ is the mass term, *i.e.* the inverse squared of the correlation length and α is a constant. In our model we find that M is linearly vanishing with doping, $M(\delta) \propto (\delta - \delta_c)$. At $\mathbf{k} = \mathbf{q_c}$, M is the distance from the criticality. In Figure 3 we report the values of $\mathbf{q_c}$ consistent with a quantum critical behavior and in the inset is shown the direction orthogonal to the stripes at varying doping for fixed values of the other parameters. We note that the direction of the stripes depends on doping similarly to what observed in some neutron scattering experiments [28,29].

Taking into account the expression (16) for the vertex function, the imaginary part of the Z function can be calculated by:

$$\mathrm{Im}Z(\mathbf{k},\omega) = \int_{-\pi/a}^{\pi/a} \frac{\mathrm{d}k'_x}{2\pi} \times \int_{-\pi/a}^{\pi/a} \frac{\mathrm{d}k'_y}{2\pi} \frac{\gamma_{k-k'}[\omega - \epsilon_{\mathbf{k}'}][n_B(\omega - \epsilon_{\mathbf{k}'}) + n_F(\epsilon_{\mathbf{k}'})]}{\Omega^2(\mathbf{k} - \mathbf{k}') + \gamma^2_{k-k'}[\omega - \epsilon_{\mathbf{k}'}]^2} A_{\mathbf{k}'} t^2_{\mathbf{k}'}. \quad (17)$$

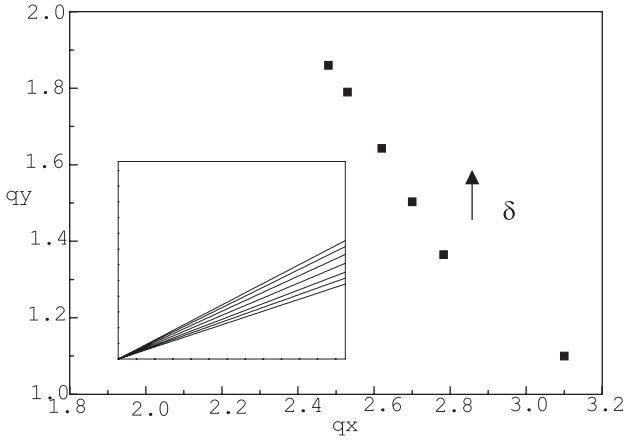

Fig. 3. The squares represent the critical vector $\mathbf{q_c} = (q_c^x, q_c^y)$ at increasing doping $\delta = (0.1, 0.15, 0.2, 0.25, 0.28, 0.3)$ from bottom to top. The other parameters are fixed as $t'/t = -0.25$, $U/t = 5$, and $U/V = 5$. The inset shows the direction orthogonal to the stripes at increasing doping from bottom to top for the same values used before.

We perform the calculation of the on the mass-shell lifetime at $T = 0$:

$$\mathrm{Im}Z(\mathbf{k},\epsilon_{\mathbf{k}}) = \int_{0 \leq \epsilon_{\mathbf{k}'} \leq \epsilon_{\mathbf{k}}} \frac{\mathrm{d}^2k'}{(2\pi)^2} \frac{\gamma^{-1}_{k-k'}[\epsilon_{\mathbf{k}} - \epsilon_{\mathbf{k}'}]}{\tilde{\Omega}^2(\mathbf{k} - \mathbf{k}') + [\epsilon_{\mathbf{k}} - \epsilon_{\mathbf{k}'}]^2} A_{\mathbf{k}'} t^2_{\mathbf{k}'}, \quad (18)$$

where we have defined $\tilde{\Omega}(\mathbf{k}) = \gamma^{-1}_{k-k'}\Omega(\mathbf{k})$. This integral can be evaluated in the same fashion as in reference [16] and the details are reported in the Appendix. Namely, the main contribution to the integral comes from the region in the $\mathbf{k}$ space where the denominator vanishes. For a given $\mathbf{k}$, the two terms in the denominator do not vanish simultaneously unless $\mathbf{k}' = \mathbf{k} - \mathbf{q_c}$, where $\mathbf{q_c}$ is the vector of the critical fluctuations that connects points of the Fermi surface where $\epsilon_{\mathbf{k}} = \epsilon_{\mathbf{k}'} = 0$ (hot-spots (HS)). The final result of the integration at the hot-spots ($\mathbf{k} = \mathbf{k_{HS}}$) yields:

$$\mathrm{Im}Z(\mathbf{k},\epsilon_{\mathbf{k}}) \simeq_{k \simeq k_{HS}} \frac{\pi\sqrt{2}|\mathbf{k_{HS}} - \mathbf{q_c}|\gamma^{-1}_{k_{HS}-q_c} A_{k_{HS}-q_c} t^2_{k_{HS}-q_c}}{a v_{k_{HS}-q_c}} \sqrt{\epsilon_{\mathbf{k}}}, \quad (19)$$

where $v_{k_{HS}-q_c}$ is the velocity of the electrons. Since in the low-energy limit $\mathrm{Re}G^0(\omega)$ goes to a constant and $\mathrm{Re}Z(\mathbf{k},\omega)$ is a regular function, the behavior of $\mathrm{Im}Z(\mathbf{k},\omega)$ determine the behavior of the inverse scattering time of quasiparticles (5) at the HS as

$$\frac{1}{\tau_{HS}} \simeq \sqrt{\epsilon_{\mathbf{k}}}. \quad (20)$$

When M is different from zero, in the small energy limit ($\epsilon_{\mathbf{k}} \ll M$), it prevents the denominator of (18) from vanishing and the usual Fermi liquid behavior is recovered $1/\tau_k \propto \epsilon_k^2$ (details are given in the Appendix). In the

regime $\epsilon_{\mathbf{k}} \gg M$ the square-root behavior still holds. This implies that along the line $\epsilon_{\mathbf{k}} = \epsilon_{\mathbf{k}-\mathbf{q_c}}$ the quantity M determines the energy scale that separates the Fermi liquid (FL) regime from the non FL one. The maximum violation of the FL behavior is obtained when $M = 0$ at the points where k approaches the Fermi surface.

3 Results

In Figure 4 the inverse scattering time calculated from equation (18) is shown as a function of the dimensionless quantity $\epsilon_{\mathbf{k}}/\epsilon_{max}$, where ϵ_{max} is given by the maximum value of the single-particle dispersion in (8), at varying M/t and for $\epsilon_{\mathbf{k}} \simeq 0$. We fix the parameters as $t'/t = -0.25$, $U/t = 5$, with the ratio $U/V = 5$, and leave the hole-doping δ as a free parameter to change the position of the Fermi level and the location of the hot spots. For each fixed doping we determine numerically the value of the characteristic wave-vector $\mathbf{q_c}$ and the hot-spots within the first Brillouin zone as the intersections between the FS and the four lines $k_y = \pm q_c/a \pm k_x$. We let M/t vary in the range $(10^{-6}; 10^{-1})$ to explore the crossover between FL-non-FL. In Figure 4 we see that as M/t is reduced, the bottom curve ($M/t = 10^{-1}$) displays a pure Fermi liquid-behavior , whereas the top curve, corresponding to $M/t = 10^{-6}$, displays a square-root non-FL behavior. The crossover curves are characterized by a *linear* behavior. The energy dependence of ImΣ in this region is consistent with recent ARPES data based on the peak width in $Bi_2Sr_2CaCu_2O_{8+\delta}$ [1]. The experiments show that for a given temperature ImΣ is constant up to some energy. At larger binding energy, ImΣ scales linearly with ω and is independent of temperature, with a behavior very different from that found in metallic systems [30,31]. We would like to stress that the same type of results have been previously obtained in a phenomenological model of electrons coupled to a fluctuating charge field whose properties are described by a correlation function of the form (16).

4 Conclusions

By using a strong coupling approach based on a Cumulant Expansion, we have analyzed the influence of a charge vertex singularity on the quasiparticles lifetime in an extended single-band Hubbard model to explain the deviation from the normal Fermi liquid behavior observed into experiments. For physical values of the parameters we have found that the charge vertex diverges at a wave vector $\mathbf{q_c}$ in a way consistent with the existence of a Quantum Critical Point at finite doping. The results of our analysis show that deviations from a conventional Fermi liquid appear in the on-shell inverse scattering time at the points of the Fermi surface connected by the characteristic wave-vectors of the critical charge fluctuations (hot-spots). We have found that the self-energy shows a linear behavior in the crossover regime induced by the doping, between a Fermi liquid, at higher doping and low temperature, where

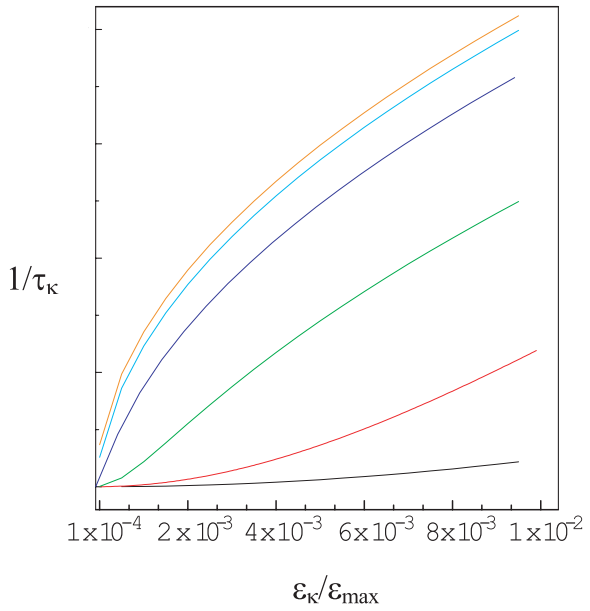

Fig. 4. The inverse of the scattering time (in arbitrary units) as a function of $\epsilon_{\mathbf{k}}/\epsilon_{max}$ at varying M/t in the range $(10^{-6}; 10^{-1})$ (from top to the bottom curve) and for $\epsilon_{\mathbf{k}} \to 0$. The parameters are fixed as $t'/t = -0.25$, $U/t = 5$, and $U/V = 5$, while we leave the hole-doping δ as a free parameter to change the position of the Fermi level and the location of the hot spots. The bottom curve ($M/t = 10^{-1}$) displays a pure Fermi liquid-behavior , whereas the top curve, corresponding to $M/t = 10^{-6}$, displays a square-root non-FL behavior.

Im$\Sigma \propto \omega^2$ and the quantum-critical regime at lower doping, where Im$\Sigma \propto \sqrt{\omega}$. The crossover between the two limits is governed by the inverse squared of the correlation length, $\xi^{-2} \sim a(\delta - \delta_c)$, that locates at $\delta = \delta_c$ a quantum critical point. These features are observed in various ARPES experiments on Bi2212. We would like to stress the microscopic derivation of our results contrasted to various phenomenological proposals present in literature. As a future work we would like to analyze the quasiparticle spectra to understand the different nature of low-energy excitations in various parts of the first Brillouin zone and understand the interplay or coexistence of superconductivity and stripe phases.

Appendix A: Evaluation of the imaginary part of Z(k,ω)

In evaluating the integral (18) we use polar coordinates, $\int \mathrm{d}^2k' \to |\mathbf{k} - \mathbf{q_c}| \int \mathrm{d}\rho \int \mathrm{d}\phi$, and along the line $\mathbf{k}' = \mathbf{k} - \mathbf{q_c}$ we expand the function $\Omega(\mathbf{k} - \mathbf{k}')$ in the following way,

$$\Omega(\mathbf{k} - \mathbf{k}') \simeq M(\delta) + a^2(|\mathbf{k} - \mathbf{q_c}|^2\phi^2 + \rho^2)/2 \qquad \text{(A.1)}$$

where a is some constant, ϕ is the angle between the vectors $\mathbf{k}', \mathbf{k} - \mathbf{q_c}$ and $\rho = |\mathbf{k}'| - |\mathbf{k} - \mathbf{q_c}| \simeq (\epsilon_{\mathbf{k}} - \epsilon_{\mathbf{k}-\mathbf{q_c}})/v_{k-q_c}$, with $\rho \ll |k - q_c|$, v_{k-q_c} is the velocity of

the electrons at the point $\mathbf{k}-\mathbf{q_c}$. Using this expansion the integral (18) becomes:

$$\mathrm{Im}Z(\mathbf{k},\epsilon_{\mathbf{k}}) \simeq \frac{|\mathbf{k_{HS}}-\mathbf{q_c}|\gamma^{-1}_{k_{HS}-q_c}A_{k_{HS}-q_c}t^2_{k_{HS}-q_c}}{v_{k_{HS}-q_c}}\int_0^{\epsilon_k}\mathrm{d}(\rho v_{k_{HS}-q_c}) \times\int_0^{\bar{\phi}}\mathrm{d}\phi\frac{\rho v_{k_{HS}-q_c}}{(\rho v_{k_{HS}-q_c})^2+(M+a^2|k_{HS}-q_c|^2\phi^2/2)^2} = \frac{|\mathbf{k_{HS}}-\mathbf{q_c}|\gamma^{-1}_{k_{HS}-q_c}A_{k_{HS}-q_c}t^2_{k_{HS}-q_c}}{v_{k_{HS}-q_c}} \times\int_0^{\infty}\mathrm{d}\phi\log\left[1+\frac{\epsilon_k^2}{(M+a^2|k_{HS}-q_c|^2\phi^2/2)^2}\right]. \quad (A.2)$$

We evaluate this integral in different regions.
At the critical point $M=0$:

$$\mathrm{Im}Z(\mathbf{k},\epsilon_{\mathbf{k}}) = \frac{|\mathbf{k_{HS}}-\mathbf{q_c}|\gamma^{-1}_{k_{HS}-q_c}A_{k_{HS}-q_c}t^2_{k_{HS}-q_c}}{v_{k-q_c}}\sqrt{2\epsilon_{\mathbf{k}}} \int_0^{\infty}\mathrm{d}\theta\log\left[1+\frac{1}{((a^2|k_{HS}-q_c|^2\theta^2)^2}\right], \quad (A.3)$$

where $\theta=\phi/\sqrt{2\epsilon_{\mathbf{k}}}$ and the upper limit is extended to ∞ to extract the leading behavior such that

$$\mathrm{Im}Z(\mathbf{k},\epsilon_{\mathbf{k}}) \simeq \frac{\pi\sqrt{2}|\mathbf{k_{HS}}-\mathbf{q_c}|\gamma^{-1}A_{k_{HS}-q_c}t^2_{k_{HS}-q_c}}{av_{k_{HS}-q_c}}\sqrt{\epsilon_{\mathbf{k}}}. \quad (A.4)$$

This is the result reported in the main text (19).

In the small energy limit ($\epsilon_{\mathbf{k}}\ll M$):

When M is different form zero, it prevents the denominator of (18) from vanishing and the usual Fermi liquid behavior is recovered $\frac{1}{\tau_k}\propto\epsilon_k^2$. In fact, the expansion of the log in the integral (A.2) in the limit $\epsilon_{\mathbf{k}}\ll M$ and small ϕ gives:

$$\log\left[1+\frac{\epsilon_k^2}{M}\frac{1}{1+\frac{a^2|k_{HS}-q_c|^2\phi^2}{2M}}\right] \simeq \log\left[1+\frac{\epsilon_k^2}{M}(1-a^2|k_{HS}-q_c|^2\phi^2/2M)\right] \simeq \log\left[1+\frac{\epsilon_k^2}{M^2}\right]-\frac{\epsilon_k^2a^2|k_{HS}-q_c|^2\phi^2}{2M^2}\simeq\frac{\epsilon_k^2}{M^2}. \quad (A.5)$$

Finally, in the regime $\epsilon_k\gg M$ the square-root behavior is recovered.

References

1. T. Valla, *et al.*, Science **285**, 2581 (1999)
2. P.W. Anderson, *The Theory of Superconductivity in the High T_c Cuprates* (Princeton University Press, Princeton, New Jersey, 1997)
3. T. Timusk, R.B. Tanner, in *Infrared Properties of High T_c superconductors*, Vol. 1 edited by M.G. Ginsberg (World Scientific, Singapore, 1988)
4. H. Takagi *et al.*, Phys. Rev. Lett. **69**, 2975 (1992)
5. Y. Ando *et al.*, Phys. Rev. Lett. **75**, 4622 (1995); Y. Ando *et al.*, Phys. Rev. Lett. **77**, 2065 (1996)
6. J.M. Tranquada *et al.*, Nature **375**, 561 (1995)
7. R.P. Sharma *et al.*, Nature **404**, 736 (2000)
8. X.J. Zhou *et al.*, Science **286**, 268 (1999)
9. H.A. Mook *et al.*, Nature **404**, 729 (2000)
10. N.L. Saini *et al.*, Phys. Rev. Lett. **79**, 3464 (1997)
11. D.S. Marshall *et al.*, Phys. Rev. Lett. **76**, 4841 (1996)
12. C. Varma *et al.*, Phys. Rev. Lett. **63**, 1996 (1989), *ibid.* **64**, 497 (1990)
13. A. Millis, H. Monien, D. Pines, Phys. Rev. B. **46**, 14803 (1990)
14. A.V. Chubukov, D.K. Morr, K.A. Shaknovich, Phil Mag. **74**, 563 (1996)
15. V.J. Emery, S.A. Kivelson, Physica C **209**, 597 (1993)
16. C. Castellani, C. Di Castro, M. Grilli, Phys. Rev. Lett. **75**, 4650 (1995); C. Castellani, C. Di Castro, M. Grilli, Z. Phys. B **103**, 137 (1997)
17. S. Sachdev, J. Ye, Phys. Rev. Lett. **69**, 2411 (1992)
18. S. Caprara, M. Sulpizi, A. Bianconi, C. Di Castro, M. Grilli, Phys. Rev. B. **59**, 14980 (1999)
19. V.A. Moskalenko, L.Z. Kon, Cond. Matt. Phys. **1**, 23 (1998)
20. W. Metzner, Phys. Rev. B **43**, 8549 (1991)
21. S. Pairault, D. Senechal, A.-M.S. Tremblay, Phys. Rev. Lett. **80**, 5389 (1998)
22. R. Citro, M. Marinaro, Eur. Phys. J. B **20**, 343 (2001).
23. R. Citro, M. Marinaro, Int. J. Mod. Phys. **14**, 3000 (2000)
24. V.M. Galitskii, JETP **34**, 279 (1958)
25. Hereafter we choose t as energy unity
26. F. Becca, M. Tarquini, M. Grilli, C. Di Castro, Phys. Rev. B **54**, 12443 (1996)
27. $V(\mathbf{k}')$ acts as an external potential that we minimize
28. K. Yamada *et al.*, Phys. Rev. B **57**, 6165 (1998)
29. S. Wakimoto *et al.*, Phys. Rev. B **60**, 769 (1999), *ibid.* **61**, 3699 (2000)
30. T. Valla, A.V. Fedorov, P.D. Johnson, S.L. Hulbert, Phys. Rev. Lett. **83**, 2085 (1999)
31. C. Olson *et al.* Phys. Rev. B **42**, 382 (1990)